International Journal of Mass Spectrometry 309 (2012) 88–96

Contents lists available at SciVerse ScienceDirect

International Journal of Mass Spectrometry

journal homepage: www.elsevier.com/locate/ijms

Analysis of free oligosaccharides by negative-ion electrospray ion trap tandem mass spectrometry in the presence of $H_2PO_4^-$ anions

Ivo Fabrik[a,b], Richard Čmelík[a,*], Janette Bobál'ová[a]

[a] Institute of Analytical Chemistry of the Academy of Sciences of the Czech Republic, v. v. i., Veveří 97, 602 00 Brno, Czech Republic
[b] Institute of Molecular Pathology, Faculty of Military Health Sciences, University of Defence, Třebešská 1575, 500 01 Hradec Králové, Czech Republic

ARTICLE INFO

Article history:
Received 27 May 2011
Received in revised form 1 September 2011
Accepted 2 September 2011
Available online 9 September 2011

Keywords:
Oligosaccharides
Mass spectrometry
Anion attachment
Fragmentation

ABSTRACT

Positive-ion mode-tandem mass spectrometry has become a frequently used tool for the structural analysis of neutral saccharides. However, their behavior in the positive-ion mode is not always adequate for oligosaccharides structure identification. Thus, fragmentation of $[M-H]^-$ or anion adducts produced in the negative-ion mode MS, offers an alternative as their fragmentation patterns provide more structure-related information. The main drawback of the negative-ion mode MS of neutral saccharides is the low sensitivity. In this study, we tested several salts as additives of saccharide samples for sensitivity improvement in the negative-ion mode. The addition of $NH_4H_2PO_4$ forming $[M+H_2PO_4]^-$ seemed to be the best choice due to a relatively high sensitivity increase in both MS and MS^n spectra. Moreover, the salt content could be monitored by the presence of phosphate clusters at high salt-saccharide ratios and salting effects could thereby be avoided. Compared to other tested salts, fragmentation spectra of phosphate adducts also contained additional fragments which improved both the certainty and accuracy of the structural identification. The $NH_4H_2PO_4$ addition was applied to collected fractions from brewing samples separation where oligosaccharides derived from starch, fructans and oligosaccharides of the raffinose family were detected and identified. Our suggested approach is a promising alternative to a more common mass spectrometric analysis of neutral oligosaccharides in the positive-ion mode or chloride or nitrate additions in the negative-ion mode.

1. Introduction

Oligosaccharides are defined as molecules composed of 2–10 monosaccharide units connected by glycosidic linkages. Either *de novo* synthesized or as products of polysaccharide degradation, they are essential for organisms. Bonded variants participate in non-covalent interactions between proteins and cells [1,2]. Free neutral oligosaccharides often serve as an available form of energetic storage [3,4]. However, several oligosaccharide species have also attracted attention in the field of human nutrition as a part of dietary fiber. In this context, they improve immunity response and help to prevent colon cancer [5–7]. Plants are one of the main sources of dietary fiber oligosaccharides for humans. Structurally diverse, plant oligosaccharides fulfill various roles in plant metabolism. For instance, the well-known prebiotics fructans act as an energy source, but they also protect the plant from abiotic stress [8] and stabilize membranes [9]. Similarly, oligosaccharides of the raffinose family (RFO) have been shown to be involved in the defense against oxidative stress and desiccation [10]. Although β-glucans are also classified as dietary fiber, their functions in plant metabolism are different. As remnants of plant cell wall polysaccharides, they could serve as danger signals for plant defense system [11]. Also dextrins, which arise from starch hydrolysis, possess dietary fiber properties to some extent [12,13]. They consist of small linear chains of glucose units, linked by α-glycosidic linkages (mostly 1→4 and to a lesser extent 1→6), whose main function is to cover an energetic demand during plant metabolic processes [14,15].

The biological activity of oligosaccharides is closely related to their structure. Unfortunately, the analytical distinction and identification of a particular oligosaccharide is possible only with many difficulties. Therefore, the combination of specific enzymatic cleavages, appropriate separation techniques, mass spectrometry (MS) and nuclear magnetic resonance is used [16–20]. Mass spectrometric analysis based on MS^n experiments is often a method of choice for oligosaccharide sequencing and glycosidic linkage identification [21]. Most studies use matrix-assisted laser desorption/ionization

Abbreviations: DP, degree of polymerization; RFO, raffinose family of oligosaccharides; MS, mass spectrometry; MALDI, matrix-assisted laser desorption/ionization; ESI, electrospray ionization; CID, collision-induced dissociation; GPB, gas-phase basicity; Hex, hexose; HPLC, high-performance liquid chromatography; ACN, acetonitrile; Glc, glucose; Gal, galactose; Fru, fructose; Mat, maltotetraose; Nys, nystose; Sta, stachyose.

* Corresponding author. Tel.: +420 532 290 216; fax: +420 541 212 113.
E-mail address: cmelik@iach.cz (R. Čmelík).

1387-3806/$ – see front matter © 2011 Elsevier B.V. All rights reserved.
doi:10.1016/j.ijms.2011.09.002

(MALDI) or electrospray ionization (ESI) in the positive-ion mode. Under these conditions, neutral saccharides form mainly $[M+Na]^+$ and $[M+K]^+$ adducts with protonated molecules as minor products [20,22,23]. In MS^n, protonated neutral saccharides fragment almost exclusively to Y and B ions (nomenclature by Domon–Costello [24]), corresponding to glycosidic linkage cleavages. However, identification of the glycosidic linkage type requires the presence of so-called cross-ring fragments. Their higher abundance could be provided by selecting alkaline metal ions adducts (e.g., $[M+Li]^+$ or $[M+Na]^+$) as precursors. When the low-energy collision-induced dissociation (CID) is used, observed cross-ring fragments correspond to A type ions. They are formed by the loss of neutral species of molecular formula $(CH_2O)_n$, where $n=1$ (^{0,2}A), 2 (^{0,3}A), and 3 (^{0,4}A and ^{2,4}A) [25,26]. By contrast, at the high-energy CID, less common ^{3,5}A or ^{1,5}X can be detected [27,28].

In the negative-ion mode, saccharides form $[M-H]^-$ based on their acidities. Deprotonated molecules preferentially provide C and B fragments of glycosidic bonds and A type cross-ring ions in the low-energy CID [25,29]. Beside $[M-H]^-$ ions, an adduct formation ($[M+X]^-$) could occur in the presence of appropriate anions (X^-). Therefore, gas-phase basicities (GPBs) of ions $[M-H]^-$ and X^- are crucial for the stability of the adduct [30]. The low value of GPB for X^- increases the probability of adduct decay to X^- and the neutral sugar molecule M (this is typical for Br^- and I^-). By contrast, high GPB causes a hydrogen transfer forming HX and $[M-H]^-$ (typical for F^-) [30,31]. The most stable adduct of halogens is $[M+Cl]^-$ due to a similar GPB of chloride and of $[M-H]^-$ [32,33]. Beside Cl^-, also NO_3^-, HSO_4^- and $H_2PO_4^-$ ions have been shown to form stable adducts with carbohydrates [34]. After the loss of HX during the fragmentation, the glycosidic linkage cleavage of neutral sugars occurs mostly from the reducing end of the gas-phase ion. This leads to the previously described fragments of $[M-H]^-$.

With regard to saccharide analysis, acceptance of the negative-ion mode is still increasing [34–36]. When appropriate conditions are set, a type of the glycosidic bond can be identified even in MS by means of in-source fragmentation [37,38]. Nevertheless, the information gathered by the fragmentation in both positive- and negative-ion modes is, to a certain extent, complementary and an accurate elucidation of structures of saccharides requires the combination of both modes.

The phenomenon of saccharide-salt adduct formation could be generally utilized for the increase of sensitivity in MS and MS^n after the addition of appropriate salt [39,40]. The aim of this study was to apply this approach in the negative-ion mode by the addition of $NH_4H_2PO_4$ to the sample and, in this way, to distinguish individual structural motifs of neutral saccharides. Free oligosaccharides present in HPLC fractions collected after the separation of real samples of plant origin were analyzed in this manner. Several studies used $[M+H_2PO_4]^-$ for the mass spectrometric analysis of oligosaccharides [41–43]. However, this was a result of sample processing rather than a goal-directed step and the full potential of the method was not exploited. The described procedure offers a promising alternative to the more common mass spectrometric analysis in the positive-ion mode, or chloride or nitrate attachment in the negative-ion mode with equal sensitivity. Due to the presence of phosphate clusters in MS spectra, negative effects of high salt content could be monitored. Moreover, the fragmentation of phosphate-sugar adducts provides more structure-specific cross-ring fragments, which facilitates the assignment of the structure.

2. Materials and methods

2.1. Chemicals and samples

All chemicals were purchased from Sigma–Aldrich (St. Louis, MO, USA) unless otherwise indicated. NH_4Cl, NH_4NO_3 and 1-kestose were purchased from Fluka (Buchs, Switzerland), $NH_4H_2PO_4$ from Lachema (Brno, Czech Republic), ethanol from Riedel-de Haën (Seelze, Germany) and acetonitrile and water of Super Gradient HPLC purity from Labscan (Gliwice, Poland). Samples of barley and malt (Jersey variety) and sweet wort, wort and green beer (Bojos variety) were obtained from the Research Institute of Brewing and Malting (Brno, Czech Republic) and stored at −20 °C.

2.2. Sample preparation

Powdered samples of barley and malt (50 mg) were suspended in 0.5 ml of deionized water or in 80% ethanol and shaken (30 min, 1000 rpm) at 55 °C (Thermomixer Comfort, Eppendorf, Hamburg, Germany). Extracts were then centrifuged (2 min, 12 000 × *g*, MiniSpin plus, Eppendorf, Hamburg, Germany) and the supernatant was kept. The pellet was again suspended in the same volume of solvent, the whole process being repeated and supernatants were combined. Samples extracted by 80% ethanol were dried and then dissolved in deionized water of a volume equal to the extraction

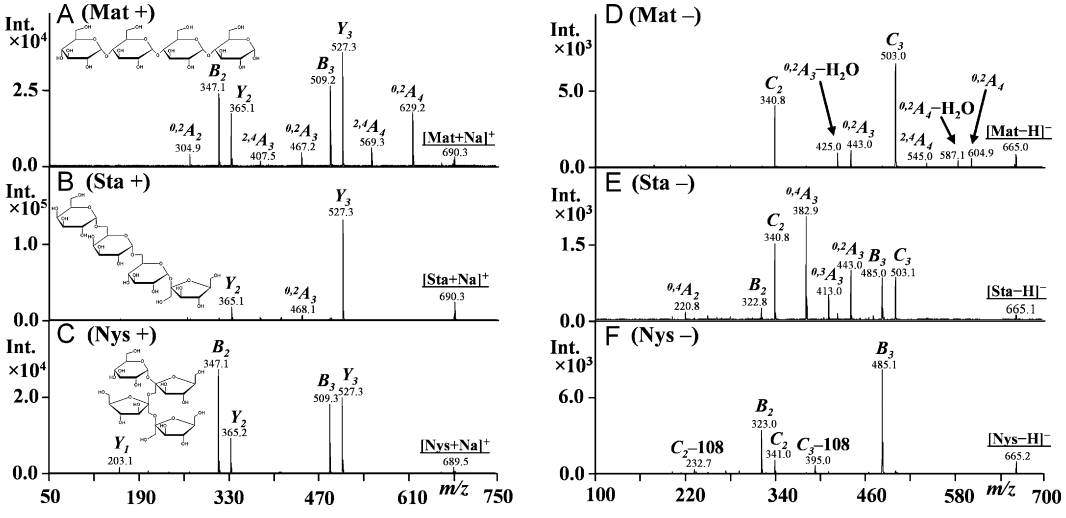

Fig. 1. MS^2 positive-ion spectra of sodium adducts of (A) maltotetraose, (B) stachyose and (C) nystose and MS^2 negative-ion spectra of deprotonated molecules corresponding to (D) maltotetraose, (E) stachyose and (C) nystose (30 μM, 50% ACN, without additives). Precursor ions are underlined.

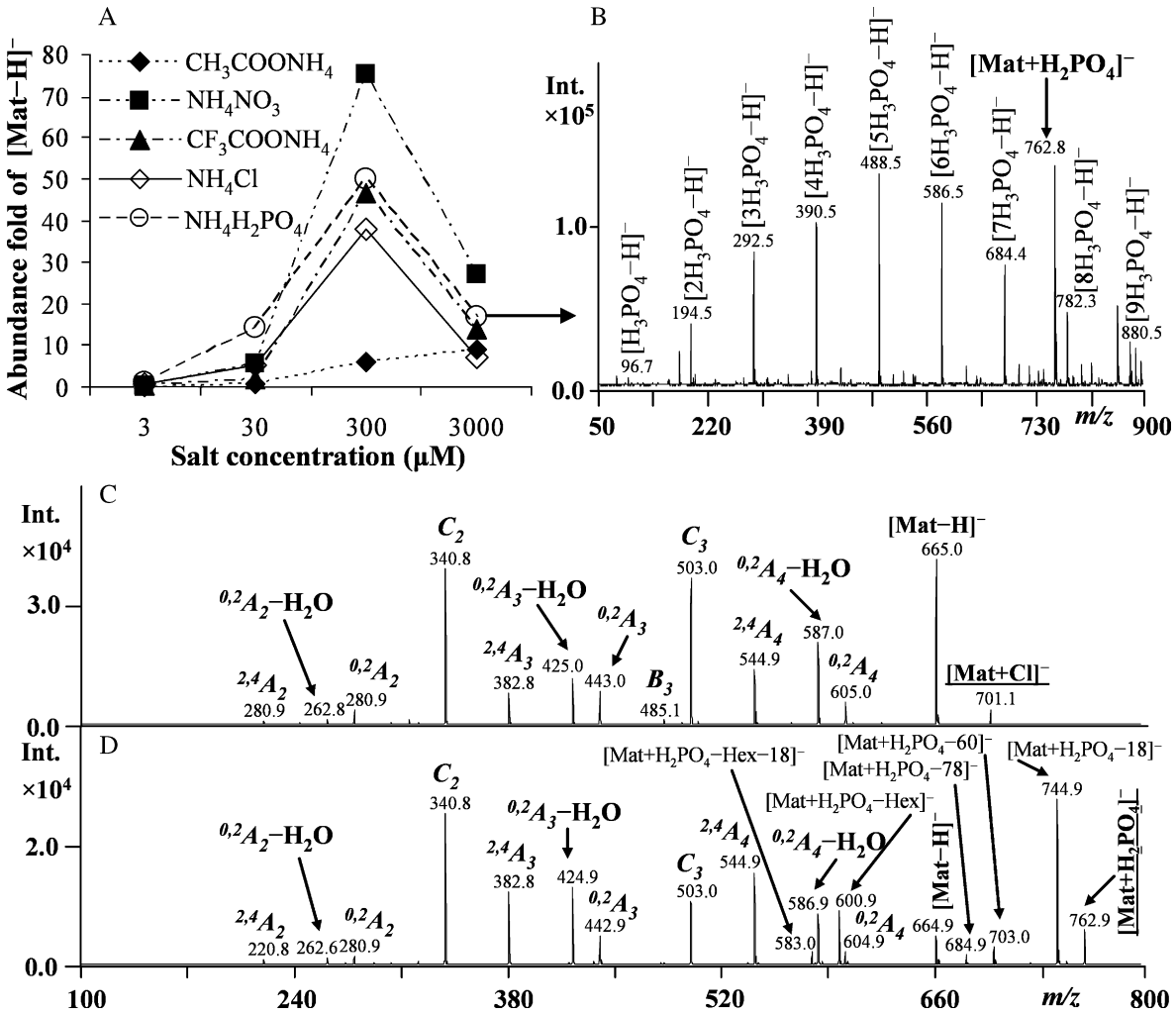

Fig. 2. (A) Effect of salt concentration on the abundance ratio of the salt adduct and $[Mat-H]^-$ without additives in the negative-ion mode (30 μM Mat in 50% ACN), (B) the negative-ion MS spectrum of $[Mat+H_2PO_4]^-$ after the addition of $NH_4H_2PO_4$ to Mat standard in a ratio 1:100 (Mat:salt, 30 μM Mat in 50% ACN); MS^2 negative-ion spectra of (C) $[Mat+Cl]^-$ and (D) $[Mat+H_2PO_4]^-$ after the addition of the corresponding ammonium salt to Mat standard solution in a ratio 1:10 (Mat:salt, 30 μM Mat in 50% ACN). Precursor ions are underlined.

solvent. Processed powdered samples (barley and malt) and untreated liquid samples (sweet wort, wort and green beer) were finally centrifuged and filtered through nylon filters (0.22 μm, Millex Millipore, Billerica, Mass. USA) before the analysis.

2.3. High-performance liquid chromatography (HPLC)

A HPLC analysis was performed on HP 1100 Series (Hewlett Packard, Palo Alto, CA, USA) with binary pump, RI detector and autosampler. Separation of saccharides was achieved on a Prevail Carbohydrate ES column (5 μm polymeric beads with polar amino-based coating, 250 × 4.6 mm i.d.) with a guard column (7.5 × 4.6 mm i.d.) (Grace Davison Discovery Sciences, Deerfield, IL, USA). All samples were analyzed using isocratic elution. For the mobile phase, 60% acetonitrile (ACN) in mixture with water (ACN:H_2O 3:2, v/v) and, for a better resolution of oligosaccharides with lower DP, 65% ACN (ACN:H_2O 13:7, v/v) were chosen. The flow rate was 1 mL min^{-1}, the sample injection was 10 μL, and the temperature of the column and the RI detector cell was kept at 35 °C. Chromatographic data were processed using Agilent ChemStation software. The mobile phase was degassed before the analysis by a sonification (15 min, Elmasonic S100, Elma, Singen, Germany). Standards were dissolved in deionized water. Separated real samples were fractionated for off-line MS analysis.

2.4. Positive-ion and negative-ion electrospray ionization–ion trap mass spectrometry

MS^n experiments were performed on an Esquire-LC mass spectrometer (Bruker Daltonics, Bremen, Germany) with ESI ion source in both positive-ion and negative-ion modes. Samples were injected by a flow rate of 3 μL min^{-1}. Standards of saccharides were dissolved in a mixture of ACN:H_2O 1:1 (v/v). Optimization of skimmer-nozzle and ion guide octopole potentials and trapping conditions for the given *m/z* was carried out for every analysis. The drying gas temperature was set on 250 °C with a flow rate of 5 L min^{-1}, the pressure of the nebulizing gas (N_2) was 100 kPa. Spectra were obtained by averaging 25 scans; the acquisition time for one scan was 200 ms. Fragmentation amplitudes were set to acquire the precursor signal at 10% of abundance of spectrum base peak.

2.5. Method performance

To evaluate of method performance the following parameters have been determined: sensitivity, linearity, and precision. We

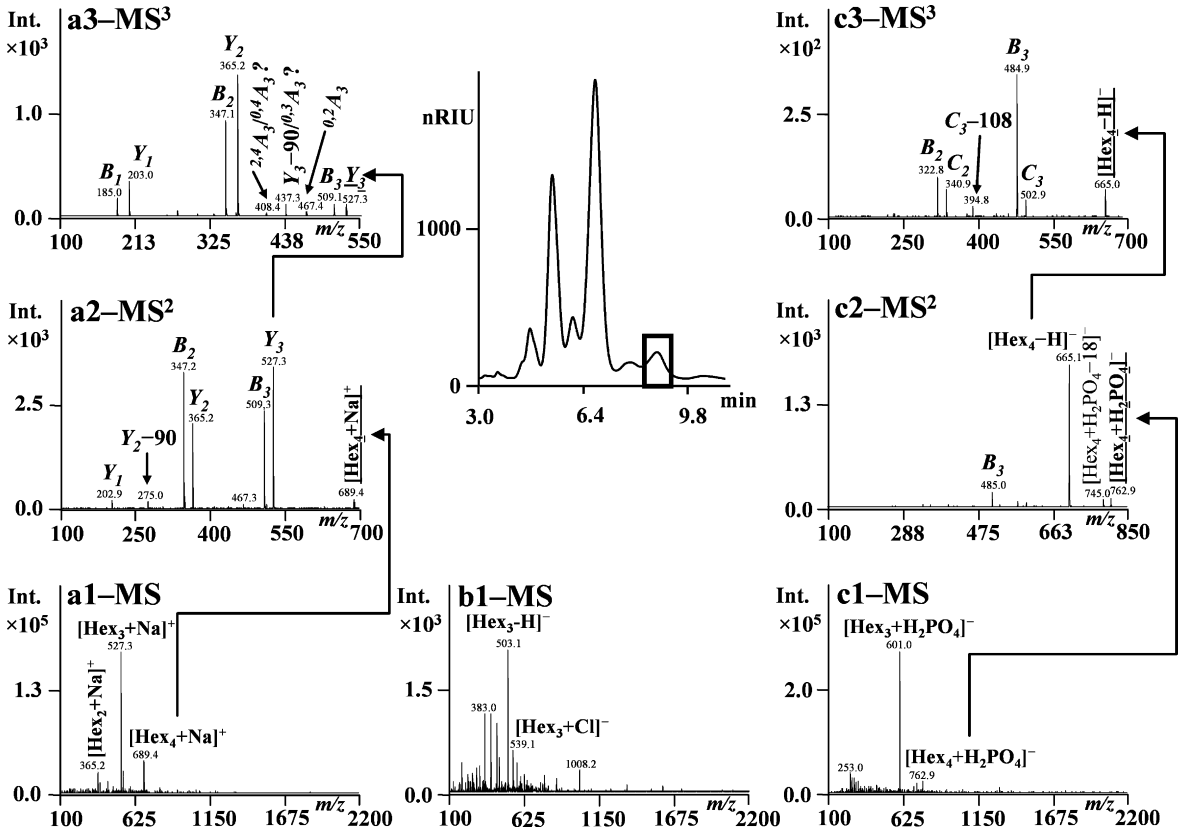

Fig. 3. The comparison of MS and MS^n analyses of fractionated water malt extract (highlighted in the chromatogram). Spectra **a1**–**a3** were acquired in the positive-ion mode, **b1** in the negative-ion mode with no additives and **c1**–**c3** in the negative-ion mode with $NH_4H_2PO_4$ addition. Precursor ions are underlined.

have analyzed Mat with and without the presence of ammonium dihydrogen phosphate with the constant ratio Mat:salt 1/10 (n/n). All the data were determined by using the deprotonated molecule or dihydrogen phosphate adduct of maltotetraose from MS spectra (data for experiments without the salt are in brackets). The concentration of Mat has been controlled in the range 0–100 μg mL^{-1}. Three replicates were analyzed for each concentration. The linearity was expressed in terms of the correlation coefficient (R^2), the plot of the response in MS spectra vs. the concentration of the standard. A linear regression was found with satisfactory linearity (R^2 = 0.9971 (0.9961), n = 6) over the range of 0.1–5.0 (0.5–20.0) μg mL^{-1}. Sensitivity was expressed by the limit of detection (LOD) and limit of quantitation (LOQ), which were defined as the lowest analyte amount with a signal-to-noise ratio of 3 and 10, respectively. The LOD and LOQ were calculated as 0.086 (0.336) μg mL^{-1}, respectively 0.286 (1.121) μg mL^{-1}. Both the repeatability and precision of the method were demonstrated by repetitive analyses six times in a single day, and the relative standard deviation values for Mat were less than 1.90 (2.11)%.

3. Results and discussion

3.1. Behavior of neutral saccharides in positive-ion and negative-ion mode MS^2

Both the positive-ion and negative-ion modes are suitable for a mass spectrometric analysis of neutral saccharides. The first is characterized by a higher sensitivity; the latter could provide the additional structural information required to analyze saccharide in MS^n experiments. In our study, we focused on neutral plant oligosaccharides. The fragmentation behavior in positive-ion and negative-ion modes was compared using standards of tetraoses maltotetraose (Mat, α-D-Glc-(1→4)-[α-D-Glc-(1→4)]$_2$-α-D-Glc), stachyose (Sta, α-D-Gal-(1→6)-α-D-Gal-(1→6)-α-D-Glc-(1↔2)-β-D-Fru) and nystose (Nys, β-D-Fru-(2→1)-β-D-Fru-(2→1)-β-D-Fru-(2↔1)-α-D-Glc) whose structural motifs could likely be found in the plant sample (Fig. 1) [44–46]. Since these standards contain several types of the glycosidic linkage, they partially cover the diverse nature of neutral plant oligosaccharide types.

Analyzed standards of maltotetraose, stachyose and nystose in the positive-ion mode preferentially formed their sodium adducts in MS spectra (not shown). Fragmentation of these adducts resulted in spectra depicted in Fig. 1A–C. It was possible to identify maltotetraose α(1→4) glycosidic linkages through to the presence of ^{0,2}A and ^{2,4}A cross-ring fragments (Fig. 1A) [25]. The situation changed when sodium adducts of non-reducing oligosaccharides were fragmented (Fig. 1B and C). Both stachyose ([Sta+Na]$^+$) and nystose ([Nys+Na]$^+$) fragmentation spectra lacked cross-ring fragments in the m/z range between the precursor adduct and Y_3. These results are consistent with the fragmentational behavior of non-reducing oligosaccharides [26]. Nevertheless, the identification of other glycosidic linkages was complicated by the low abundance of cross-ring fragments (stachyose, Fig. 1B) or even by their absence (nystose, Fig. 1C). The MS^2 spectrum of [Sta+Na]$^+$ is dominated by Y-type fragments (Y_3 and Y_2); cross-ring fragments with a reasonable abundance (S/N = 3) were represented only by $^{0,2}A_3$. Fragmentation of sodiated stachyose adducts usually results in the appearance of ^{0,2}A, ^{0,3}A and ^{0,4}A cross-rings corresponding to α(1→6) glycosidic linkage [26]. However, as seen in the case of non-reducing stachyose (Fig. 1B), their abundance was very low and therefore the glycosidic linkage type identification would be doubtful. This kind of fragmentational behavior is even more pronounced for sodiated fructan nystose (Fig. 1C). Beside Y and B, there was complete

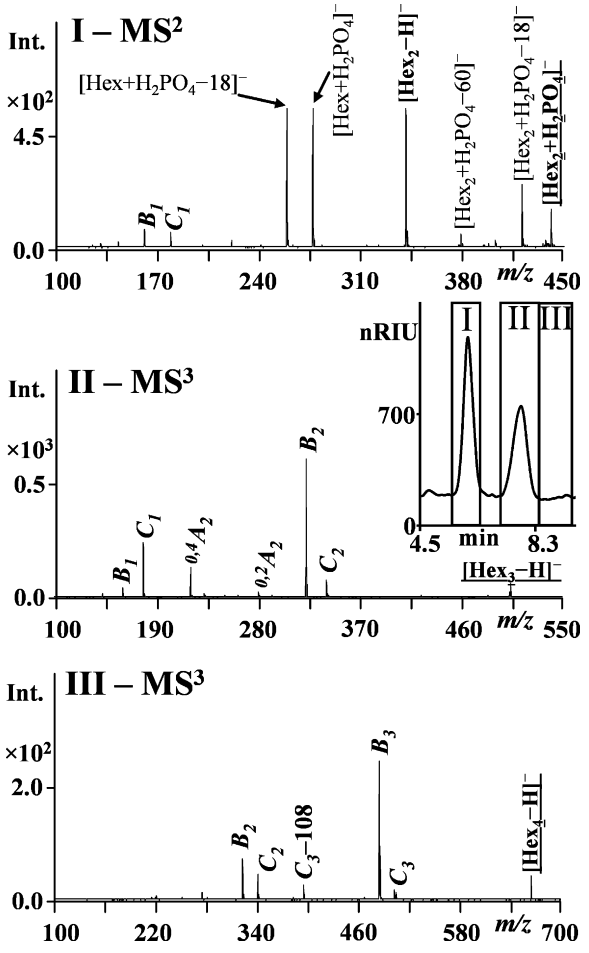

Fig. 4. MS^n analyses of HPLC fractions (I–III) of barley sample extracted by 80% ethanol with the addition of $NH_4H_2PO_4$ after collection. Precursor ions are underlined.

absence of any other fragments and the information regarding the glycosidic linkage type was lost. We were able to detect signals of ions nominally identical with the loss of 90 u from Y [47] (in some cases accompanied by minor Y−60 and Y−120), however, that was only when MS^n ($n \geq 3$) experiments were performed (not shown). It appears that the positive-ion mode suffers from the relatively low abundance of cross-rings when sodiated non-reducing oligosaccharides are fragmented. In our experiments, this was more obvious with the increasing oligosaccharide DP. Moreover, the fragmentation of alkali metal adducts of different saccharides in the positive-ion mode often provide a mixture of isobaric cross-rings formed by the loss of 60 u (^{0,2}A), 90 u (^{0,3}A for α(1→6) or Y−90 for β(2→1) of fructans) and 120 u (^{2,4}A for α(1→4) or ^{0,4}A for α(1→6)) [26,47], which further complicates the interpretation of the spectra.

In parallel to the positive-ion mode, maltotetraose, stachyose and nystose were analyzed in the negative-ion mode. All three standards gave the dominant signal of their deprotonated molecule in MS spectra (not shown). Fragmentation of $[M-H]^-$ ions of maltotetraose ($[Mat-H]^-$), stachyose ($[Sta-H]^-$) and nystose ($[Nys-H]^-$) resulted in the MS^2 spectra shown in Fig. 1D–F. Ions of C-/B- and A-type, originating from glycosidic linkage or saccharide ring cleavage respectively, were present. The MS^2 spectrum of deprotonated maltotetraose (Fig. 1D) showed a cross-ring fragment pattern typical for α(1→4) glycosidic linkage, namely the presence of ^{0,2}A, ^{0,2}A−H_2O and ^{2,4}A ions [25,38]. As with sodium adducts in the positive-ion mode, fragmentation of deprotonated stachyose and nystose did not provide any cross-ring fragments with *m/z* higher than C_3 due to their non-reducing nature (Fig. 1E and F) [29]. In contrast to the positive-ion mode, clear improvement is evident in the meaning of the presence and the abundance of cross-rings specific for the rest of glycosidic linkages present in non-reducing oligosaccharide molecules (cf. Fig. 1B with E and Fig. 1C with F). Stachyose was identified in accordance with abundant cross-rings of α(1→6) bond – ^{0,2}A, ^{0,3}A and mainly dominant ^{0,4}A (Fig. 1E) [37]. The benefits of the negative-ion mode are even more evident from the MS^2 spectrum of deprotonated nystose (Fig. 1F). When compared to the positive-ion mode with complete absence of cross-rings in the MS^2, 2→1 bond of fragmented $[Nys-H]^-$ provided minor but specific ion signals with nominal masses corresponding to C−108; here C_3−108 (*m/z* 395.0) and C_2−108 (*m/z* 232.7); see Fig. 1F.

Taken together, when considering tandem mass spectrometric analysis of model non-reducing oligosaccharides stachyose and nystose, the fragmentational behavior of deprotonated molecules provided more glycosidic linkage-related information when compared with sodiated adducts of the same molecules due to very low abundance of relevant cross-ring fragments in positive-ion mode. On the other hand, fragmentation of $[Sta-H]^-$ (Fig. 1E) and $[Nys-H]^-$ (Fig. 1F) in the negative-ion mode resulted in the presence of cross-ring patterns specific for glycosidic linkages of these non-reducing tetraoses. Moreover, tested tetraose standards (maltotetraose, stachyose and nystose) yielded in MS^2 fragments nominally specific for their different glycosidic linkages, i.e., ^{0,2}A-H_2O for α(1→4) (loss of 78 u from C, Fig. 1D), ^{0,3}A for α(1→6) (loss of 90 u from C, Fig. 1E) and C−108 for β(2→1) of fructans (loss of 108 u from C, Fig. 1F). Therefore, unlike the positive-ion mode, it would be possible to detect these types of linkages in the isobaric mixture using the negative-ion mode.

3.2. The effect of adding selected salts on the response of neutral saccharides in MS and MS^n in the negative-ion mode

A serious problem in the negative-ion mode analysis of neutral saccharides is low sensitivity, which is strongly dependent on pre-set ionization conditions. A possible solution could be the addition of appropriate salt to form the saccharide-anion adduct. In this regard, Cl^- and NO_3^- are often used [32,34]. In this study, comparing the ammonium salts additions (CH_3COONH_4, CF_3COONH_4, NH_4NO_3, NH_4Cl and $NH_4H_2PO_4$) to the 30 μM standard of maltotetraose in ratios 10:1, 1:1, 1:10 and 1:100 (Mat:salt, n/n) was made in terms of saccharide signal improvement in the negative-ion mode. The abundance of Mat-anion adducts in MS was compared with the abundance of Mat deprotonated molecule in MS without additives. The graph in Fig. 2A indicates that the addition of CH_3COONH_4 did not result in a significant increase of sensitivity compared to the non-salted Mat standard. Due to the basic character of acetate, the increase of $[Mat-H]^-$ abundance (approximately 15×) was also observed. However, this was not a significant result compared to the effects of the other salts. The optimal ratio of the other additives was shown to be 1:10 (Mat:salt). With a higher salt concentration, the sensitivity in MS dropped rapidly, probably due to the salting effects [48]. The highest response was achieved by the addition of NH_4NO_3 ($[Mat+NO_3]^-$ adducts). The signal in MS increased 75× compared to the non-treated standard of Mat. Further, signal increase was also prominent with the addition of $NH_4H_2PO_4$ ($[Mat+H_2PO_4]^-$, 50×), CF_3COONH_4 ($[Mat+CF_3COO]^-$, 47×) and NH_4Cl ($[Mat+Cl]^-$, 38×). Although the high salt content (1:100, Mat:salt) reduced the abundance of Mat adduct signals in MS, only the addition of $NH_4H_2PO_4$ in such high amounts resulted in salt-originating clusters ($[xH_3PO_4-H]^-$, x = 1–9) observation ($[Mat+H_2PO_4]^-$, *m/z* range 50–900; see Fig. 2B). An appearance of these ion clusters may indicate a crossing of the thin salt concentration line between an increase in sensitivity and salting effects.

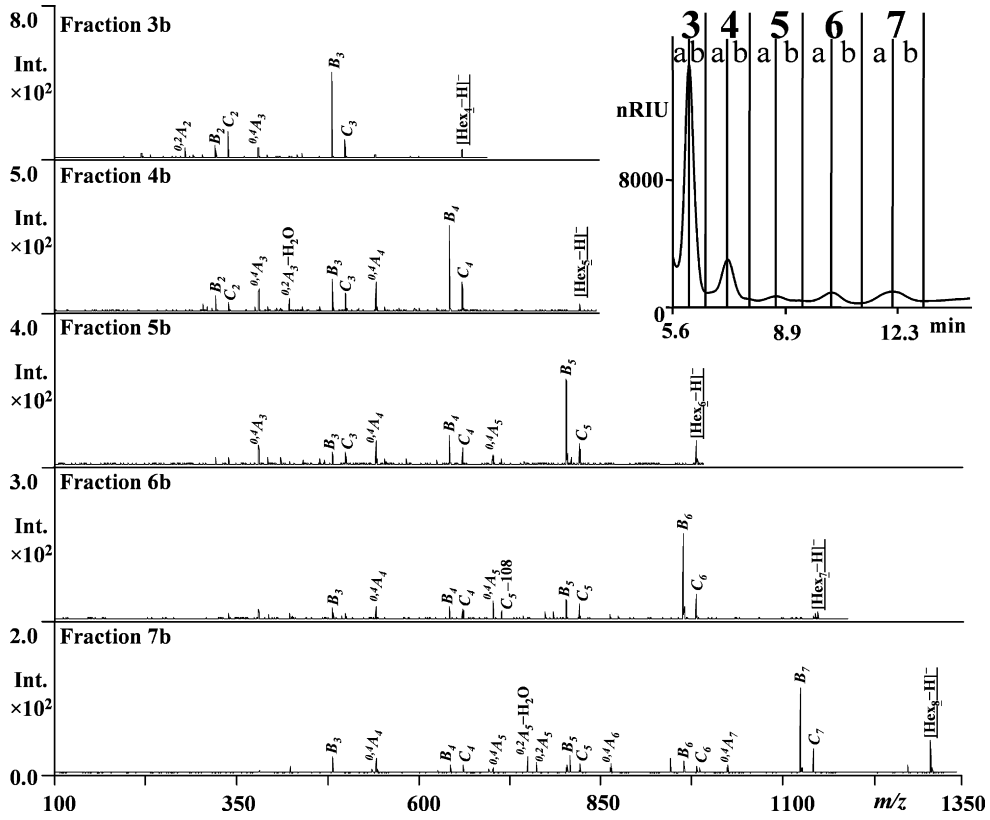

Fig. 5. MS^3 spectra of fractions denoted as **b** in the chromatogram after the addition of $NH_4H_2PO_4$. Fragments are originating from deprotonated molecules, whose precursors were minor signals of adducts $[Hex_{n+1}+H_2PO_4]^-$ detected in MS (where *n* is the number of the fraction or DP of the saccharide giving the most abundant signal in the fraction respectively). Precursor ions are underlined.

Thus, further $NH_4H_2PO_4$ addition would not improve sensitivity and may even cause its loss. This would be important especially for the optimal salt addition to real samples with unknown amounts of saccharides.

Anionic adducts of Mat and trifluoroacetate ($[Mat+CF_3COO]^-$), nitrate ($[Mat+NO_3]^-$), chloride ($[Mat+Cl]^-$) and dihydrogen phosphate ($[Mat+H_2PO_4]^-$) were fragmented. Considering the α(1→4) glycosidic linkage as a typical feature of maltooligosaccharides, the MS^2 spectrum of $[Mat–H]^-$ contained expected cross-ring fragments ($^{0,2}A$, $^{0,2}A–H_2O$ and $^{2,4}A$), however with a relatively low abundance in comparison with C type ions (Fig. 1D). All fragmentation spectra of tested Mat adducts nominally gave the same signals as the Mat deprotonated molecule (for simplicity only MS^2 spectra of $[Mat+Cl]^-$ and $[Mat+H_2PO_4]^-$ are presented in Fig. 2C and D respectively) but with relatively higher abundances. The intensity of the base peak in MS^2 was amplified by approximately 4× following the addition of CF_3COONH_4, and after adding NH_4NO_3 and $NH_4H_2PO_4$ by approximately 13× but more than 20× regarding NH_4Cl when compared to non-treated Mat. Importantly, also abundances of linkage-specific cross-ring fragments increased after the addition of salts. Besides the expected ions originating from deprotonated molecule, the fragmentation spectra of $[Mat+H_2PO_4]^-$ also contained ions derived from the phosphate adduct (Fig. 2D): $[Mat+H_2PO_4–18]^-$ (or $B_4+H_3PO_4$), $[Mat+H_2PO_4–60]^-$ (or $^{0,2}A_4+H_3PO_4$), $[Mat+H_2PO_4–78]^-$ (or $^{0,2}A_4$-H_2O+H_3PO_4), $[Mat+H_2PO_4–Hex]^-$ (or $C_3+H_3PO_4$) and $[Mat+H_2PO_4–Hex–18]^-$ (or $B_3+H_3PO_4$). With respect to the α(1→4) glycosidic linkage, cross-ring fragments originating from the phosphate adduct showed a pattern analogous to those from $[Mat–H]^-$ (cf. Figs. 1D and 2D) and as such, they can improve both the certainty and accuracy of the saccharide structural analysis.

Besides Mat, the addition of salts was tested on non-reducing standards of stachyose and nystose whose structural motifs could be found in high amounts in the plant material. Fragmentation of $[Sta+X]^-$ and $[Nys+X]^-$ (X = CF_3COO, NO_3, Cl, H_2PO_4) generated almost exclusively deprotonated molecules of stachyose and nystose, respectively (shown only for phosphate adduct of nystose for simplicity, see Fig. S1B). In our experiments, this was typical fragmentational behavior of all non-reducing oligosaccharides tested, independent of their DP (except sucrose; see below). Therefore, the detailed structural analysis of non-reducing saccharides salt adducts was possible only by performing MS^3 with deprotonated molecules as precursor for the third stage (Fig. S1C). The disadvantageous utilization of MS^3 for the salt addition approach (when non-reducing oligosaccharides are analyzed) is compensated by a dramatic increase in the sensitivity of the negative-ion mode. Moreover, the reducing and non-reducing nature of analyzed oligosaccharides was easily distinguished. Nevertheless, MS^3 makes high demands on sufficient yields of deprotonated molecules in the second stage. In our experiments, the efficiency in generating $[M–H]^-$ in MS^2 from non-reducing oligosaccharide adducts varied with the added salt type used (not shown) from relatively low yields (observed for CF_3COO^- and NO_3^- adducts, with $[M–H]^-$ abundance of few hundredths of MS adducts signals) to intensities of several tenths of MS precursor (for Cl^- and $H_2PO_4^-$ adducts).

Based on the results of experiments conducted on reducing and non-reducing neutral saccharides, $NH_4H_2PO_4$ was chosen as the additive for MS^n in the negative-ion mode of real samples. $H_2PO_4^-$ adducts of tested standards were detected in relatively high yields in MS (Fig. 2A) and provided relatively abundant signals in MS^2 (Fig. 2D and S1B), which is important especially for non-reducing saccharides. Moreover, as mentioned above, the use of $NH_4H_2PO_4$

had the advantage of controlling the optimal amount of added salt (and therefore maintaining high sensitivity) and the presence of additional cross-ring fragments in MS^2 spectra facilitated the structural identification of reducing neutral saccharides.

3.3. Off-line negative-ion MS^n analysis of brewing samples fractions with the addition of $NH_4H_2PO_4$

The major part of the brewing samples consists of neutral oligosaccharides [46,49]. In this study, their MS^n analysis was improved by the addition of $NH_4H_2PO_4$ to the sample. After their separation on the amino column (see Section 2.3), fractions of barley and malt extracts, as well as sweet wort, wort and green beer were collected. Following the addition of $NH_4H_2PO_4$ to fractions, their off-line negative-ion MS^n analysis was performed.

First, to assess the sensitivity and structure-related informative value of this approach, a fraction of water-extracted malt with retention time of maltotriose was chosen for the mass spectrometric comparison. Following the fraction collection, off-line analyses in the positive-ion mode (Fig. 3-a1), in the negative-ion mode (Fig. 3-b1) without additives and in the negative-ion mode with the addition of $NH_4H_2PO_4$ (Fig. 3-c1) were performed. Malt is relatively rich for diverse saccharide types because of the utilization of polysaccharides during malting processes and it was very likely that more oligosaccharides would be present in the maltotriose fraction. As expected, the dominant signal corresponded to triose independently on the ion mode or the salt addition (the positive-ion mode: $[Hex_3+Na]^+$, the negative-ion mode: $[Hex_3-H]^-$, the negative-ion mode with $NH_4H_2PO_4$ addition: $[Hex_3+H_2PO_4]^-$; Fig. 3-a1, 3-b1 or 3-c1, respectively). To compare ion-modes, minor signals of tetraose was chosen: $[Hex_4+Na]^+$ or $[Hex_4+H_2PO_4]^-$, respectively (Fig. 3-a1 or 3-c1, respectively). Due to a low sensitivity, a corresponding signal was not detected in the negative-ion mode without additives. The fragmentation of $[Hex_4+Na]^+$ in the positive-ion mode resulted in a MS^2 spectrum (Fig. 3-a2) with an intensive signal of Y and B type ions which indicated hexose-containing oligosaccharide, probably of a non-reducing nature. The glycosidic linkage types could not be identified due to the low abundance of cross-ring cleavages (cf. Fig. 1B and C). Cross-ring fragments in the *m/z* range between Y_3 and Y_2 were observed in higher intensities after the fragmentation of the Y_3 ion. However, their *m/z* 467.4, 437.3 and 408.4 – which corresponds to $^{0,2}A$, Y_3-90 and $Y_3-\times120$ – did not allow us to determine whether this tetraose contained $\alpha(1\rightarrow6)$ bond ($^{0,2}A$, $Y_3-90 = {}^{0,3}A$ and $Y_3-120 = {}^{0,4}A$), or if it was a mixture of isobaric oligosaccharides with $\alpha(1\rightarrow4)$ bonds ($^{0,2}A$ and $Y_3\text{-}120 = {}^{2,4}A$), $\beta(2\rightarrow1)$ bonds (fructans, Y_3-90) or $\alpha(1\rightarrow6)$ bond (Fig. 3-a3). On the other hand, the MS^2 spectrum of $[Hex_4+H_2PO_4]^-$ was dominated by $[Hex_4-H]^-$ (Fig. 3-c2), which is a typical feature of non-reducing saccharides (cf. reducing Mat in Fig. 2D and non-reducing nystose in Fig. S1B). The fragmentation of the deprotonated molecule confirmed the non-reducing nature of saccharide (the absence of cross-ring fragments in the *m/z* range between $[Hex_4-H]^-$ and C_3; Fig. 3-c3). The cross-ring fragment C_3-108 is specific for $\beta(2\rightarrow1)$ the glycosidic linkage of fructans (Fig. 1F). Therefore, the analyzed tetraose could be considered as the non-reducing fructooligosaccharide nystose. This experiment indicated that the addition of $NH_4H_2PO_4$ can enhance the sensitivity of the negative-ion mode to a level comparable to the positive-ion mode with the preservation of the advantageous features of the negative-ion mode for mass spectrometric analysis of neutral oligosaccharides. Using this approach, all brewing samples were analyzed with special emphasis on the absence of $[xH_3PO_4-H]^-$ clusters in MS after the addition of $NH_4H_2PO_4$ to ensure optimal saccharide adduct yields (see Section 3.2, Fig. 2B).

The method described was applied on HPLC fractions of barley (Fig. 4) and malt (Fig. S2) samples (both 80% ethanol extracts). In both cases, only oligosaccharides composed of hexoses were detected. The MS^2 spectrum of $[Hex_2+H_2PO_4]^-$ from barley fraction I did not show any cross-ring fragments (Fig. 4-I) and therefore this disaccharide was considered as a sucrose. Phosphate adducts from remaining barley fractions II and III produced predominantly deprotonated molecules in MS^2 (not shown). This, together with the absence of relevant cross-rings in MS^3 (Fig. 4-II and 4-III), confirmed their non-reducing nature (cf. Fig. S1). However, the presence of fragments $^{0,4}A_2$ (Fig. 4-II) and C_3-108 (Fig. 4-III) in MS^3 spectra suggested different structural features of $\alpha(1\rightarrow6)$ containing RFO raffinose (cf. Fig. 1E) and $\beta(2\rightarrow1)$ containing nystose (cf. Fig. 1F), respectively. In contrast to barley, a more diverse oligosaccharide pattern was revealed in malt fractions. Besides sucrose (Fig. S2-I; cf. Fig. 4-I) and raffinose (Fig. S2-III; cf. Fig. 4-II), also RFO with higher DP were detected according to their cross-rings (stachyose – Fig. S2-V; verbascose – Fig. S2-VII; cf. Fig. 1E). Moreover, maltooligosaccharides maltose (Fig. S2-II), maltotriose (Fig. S2-IV) and maltotetraose (Fig. S2-VI) were identified in MS^2 (note also $[Hex_n+H_2PO_4-60]^-$ and $[Hex_n+H_2PO_4-78]^-$ fragments typical for $\alpha(1\rightarrow4)$; cf. Fig. 2D).

Fractions of sweet wort, wort and green beer were due to the high content of maltose collected starting with the peak, whose retention time corresponded to maltotriose. Because results obtained for sweet wort, wort and green beer were similar, only sweet wort fractions are presented in this study. For a more detailed mass spectrometric analysis, every chromatographic signal was divided into two fractions designated as **a** and **b** (see chromatogram in Fig. S3 or Fig. 5). The number of the fraction corresponds to the DP of the saccharide, to which the dominant signal $[Hex_n+H_2PO_4]^-$ in the fraction is related. The dominant saccharide group of brewing samples are maltodextrins [49] which was confirmed by the MS^2 spectra of **a** type fractions (Fig. S3). A cross-ring pattern reflected the behavior of maltooligosaccharides with additional $[Hex_n+H_2PO_4-60]^-$ in the cases of fractions 3**a** and 4**a** (cf. Fig. 2D). The decrease of phosphate adducts fragments abundance in MS^2 spectra was observed with increasing DP. The only exception was $[Hex_n+H_2PO_4-18]^-$ with inverse trends forming the base peaks in MS^2 spectra of fractions 8**a** and 9**a**. The same phosphate adducts dominated in both the **a** and **b** type fractions MS spectra, which was proved by their fragmentation (not shown). Contrary to **a** type fractions, minor signals of phosphate adducts of saccharides with DP = (fraction number) + 1 were detected. MS^2 spectra obtained after their dissociation contained the dominant signal of the deprotonated molecule (not shown) and at fractions 3**b**–7**b** having sufficient abundance to perform a MS^3 analysis (Fig. 5). In this way, the non-reducing character was confirmed and, based on major cross-ring fragments of $^{0,4}A$ type, these oligosaccharides could probably be classified as RFO (cf. Fig. 1E). However, the occasional presence of $^{0,2}A-H_2O$ (MS^3 spectra of fractions 4**b** and 7**b**) and C_5-108 (MS^3 spectrum of fraction 6**b**) signalizes the complex structural nature of isobaric saccharides, which were not sufficiently separated by the amino column. Nevertheless, a similarly detailed analysis in the positive-ion mode was almost impossible due to the generally low abundance or even the absence of cross-ring fragments in the MS^n spectra and the lower sensitivity in MS, especially for neutral oligosaccharides with a higher DP.

4. Conclusion

In this study, we proved that the addition of an appropriate salt prior to MS^n experiments could overcome the problem of a low sensitivity of the negative-ion mode concerning the analysis of neutral oligosaccharides. At the same time, this helps to preserve the high informational value of the fragmentational behavior, which is important for structural elucidation. On the basis of experiments

conducted with standards of different structural types of neutral oligosaccharides, the addition of $NH_4H_2PO_4$ was chosen, resulting in the $[M+H_2PO_4]^-$ adducts observation. The formation of these complexes was relatively structure-independent and provided high yields of precursor ions. The presence of $[xH_3PO_4-H]^-$ clusters in the MS spectra could indicate exceeding the optimum added salt content and the loss of sensitivity, which is important especially for samples with unknown saccharide concentrations. The dissociation of $[M+H_2PO_4]^-$ led to cross-ring fragments with higher abundances compared to dissociation of deprotonated molecules. Moreover, the higher number of fragments originating from both the deprotonated molecule and directly from the phosphate adduct provided more certain and accurate structure identification. This approach was applied successively to fractions collected from the HPLC separation of brewing samples and the presence of diverse neutral oligosaccharides was confirmed by the structural identification. The suggested $NH_4H_2PO_4$ addition, with mentioned advantages, is valuable for the structural analysis of low-abundant neutral saccharides present in real samples by the negative-ion tandem mass spectrometry. This ion mode could not be applied due to the lack of sensitivity and the presence of noise in the spectra.

Acknowledgment

This work was supported from the project No. 2B06037 of Ministry of Education, Youth and Sports, Czech Republic, and by the Institutional Research Plan AV0Z40310501.

Appendix A. Supplementary data

Supplementary data associated with this article can be found, in the online version, at doi:10.1016/j.ijms.2011.09.002.

References

[1] R.A. Dwek, Glycobiology: toward understanding the function of sugars, Chem. Rev. 96 (1996) 683–720.
[2] A. Varki, Biological roles of oligosaccharides – all of the theories are correct, Glycobiology 3 (1993) 97–130.
[3] O. Kotting, J. Kossmann, S.C. Zeeman, J.R. Lloyd, Regulation of starch metabolism: the age of enlightenment? Curr. Opin. Plant Biol. 13 (2010) 321–329.
[4] J. Farrar, C. Pollock, J. Gallagher, Sucrose and the integration of metabolism in vascular plants, Plant Sci. 154 (2000) 1–11.
[5] G.R. Gibson, M.B. Roberfroid, Dietary modulation of the human colonic microbiota – introducing the concept of prebiotics, J. Nutr. 125 (1995) 1401–1412.
[6] G. Kelly, Inulin-type prebiotics – a review: Part 1, Altern. Med. Rev. 13 (2008) 315–329.
[7] C.S. Brennan, L.J. Cleary, The potential use of cereal (1→3,1→4)-beta-D-glucans as functional food ingredients, J. Cereal Sci. 42 (2005) 1–13.
[8] D.P. Livingston, D.K. Hincha, A.G. Heyer, Fructan and its relationship to abiotic stress tolerance in plants, Cell. Mol. Life Sci. 66 (2009) 2007–2023.
[9] R. Valluru, W. Lammens, W. Claupein, W. Van den Ende, Freezing tolerance by vesicle-mediated fructan transport, Trends Plant Sci. 13 (2008) 409–414.
[10] W. Van den Ende, R. Valluru, Sucrose, sucrosyl oligosaccharides, and oxidative stress: scavenging and salvaging? J. Exp. Bot. 60 (2009) 9–18.
[11] M. John, H. Rohrig, J. Schmidt, R. Walden, J. Schell, Cell signaling by oligosaccharides, Trends Plant Sci. 2 (1997) 111–115.
[12] J.L. Slavin, V. Savarino, A. Paredes-Diaz, G. Fotopoulos, A review of the role of soluble fiber in health with specific reference to wheat dextrin, J. Int. Med. Res. 37 (2009) 1–17.
[13] A. Sharma, B.S. Yadav, Ritika, resistant starch: physiological roles and food applications, Food Rev. Int. 24 (2008) 193–234.
[14] J.E. Georg-Kraemer, E.C. Mundstock, S. Cavalli-Molina, Developmental expression of amylases during barley malting, J. Cereal Sci. 33 (2001) 279–288.
[15] M. Gupta, N. Abu-Ghannam, E. Gallaghar, Barley for brewing: characteristic changes during malting, brewing and applications of its by-products, Compr. Rev. Food. Sci. Food Saf. 9 (2010) 318–328.
[16] A.J. Mort, M.L. Pierce, Preparation of carbohydrates for analysis by modern chromatography and electrophoresis, in: Z. El Rassi (Ed.), Carbohydrate Analysis by Modern Chromatography and Electrophoresis, Elsevier Science Bv, Amsterdam, 2002, pp. 3–38.
[17] N. Takahashi, Multi-dimensional mapping of *N*-linked glycans by HPLC, in: Z. El Rassi (Ed.), Carbohydrate Analysis by Modern Chromatography and Electrophoresis, Elsevier Science Bv, Amsterdam, 2002, pp. 347–385.
[18] T. Endo, Lectin-affinity chromatography of carbohydrates, in: Z. El Rassi (Ed.), Carbohydrate Analysis by Modern Chromatography and Electrophoresis, Elsevier Science Bv, Amsterdam, 2002, pp. 251–265.
[19] E.F. Hounsell, H-1 NMR in the structural and conformational analysis of oligosaccharides and glycoconjugates, Prog. Nucl. Magn. Reson. Spectrosc. 27 (1995) 445–474.
[20] J. Zaia, Mass spectrometry of oligosaccharides, Mass Spectrom. Rev. 23 (2004) 161–227.
[21] D. Ashline, S. Singh, A. Hanneman, V. Reinhold, Congruent strategies for carbohydrate sequencing. 1. Mining structural details by MS^n, Anal. Chem. 77 (2005) 6250–6262.
[22] D.J. Harvey, Matrix-assisted laser desorption/ionization mass spectrometry of carbohydrates, Mass Spectrom. Rev. 18 (1999) 349–450.
[23] D.J. Harvey, Matrix-assisted laser desorption ionisation mass spectrometry of oligosaccharides and glycoconjugates, J. Chromatogr. A 720 (1996) 429–446.
[24] B. Domon, C.E. Costello, A systematic nomenclature for carbohydrate fragmentations in FAB-MS/MS spectra of glycoconjugates, Glycoconjugate J. 5 (1988) 397–409.
[25] S. Pasanen, J. Janis, P. Vainiotalo, Cello-, malto- and xylooligosaccharide fragmentation by collision-induced dissociation using QIT and FT-ICR mass spectrometry: a systematic study, Int. J. Mass Spectrom. 263 (2007) 22–29.
[26] M.R. Asam, G.L. Glish, Tandem mass spectrometry of alkali cationized polysaccharides in a quadrupole ion trap, J. Am. Soc. Mass Spectrom. 8 (1997) 987–995.
[27] Y. Mechref, M.V. Novotny, C. Krishnan, Structural characterization of oligosaccharides using MALDI-TOF/TOF tandem mass spectrometry, Anal. Chem. 75 (2003) 4895–4903.
[28] A. Devakumar, M.S. Thompson, J.P. Reilly, Fragmentation of oligosaccharide ions with 157 nm vacuum ultraviolet light, Rapid Commun. Mass Spectrom. 19 (2005) 2313–2320.
[29] J.A. Carroll, D. Willard, C.B. Lebrilla, Energetics of cross-ring cleavages and their relevance to the linkage determination of oligosaccharides, Anal. Chim. Acta 307 (1995) 431–447.
[30] Y. Cai, M.C. Concha, J.S. Murray, R.B. Cole, Evaluation of the role of multiple hydrogen bonding in offering stability to negative ion adducts in electrospray mass spectrometry, J. Am. Soc. Mass Spectrom. 13 (2002) 1360–1369.
[31] B. Guan, R.B. Cole, MALDI linear-field reflectron TOF post-source decay analysis of underivatized oligosaccharides: determination of glycosidic linkages and anomeric configurations using anion attachment, J. Am. Soc. Mass Spectrom. 19 (2008) 1119–1131.
[32] Y. Cai, Y. Jiang, R.B. Cole, Anionic adducts of oligosaccharides by matrix-assisted laser desorption/ionization time-of-flight mass spectrometry, Anal. Chem. 75 (2003) 1638–1644.
[33] J. Zhu, R.B. Cole, Ranking of gas-phase acidities and chloride affinities of monosaccharides and linkage specificity in collision-induced decompositions of negative ion electrospray-generated chloride adducts of oligosaccharides, J. Am. Soc. Mass Spectrom. 12 (2001) 1193–1204.
[34] D.J. Harvey, Fragmentation of negative ions from carbohydrates. Part 1: use of nitrate and other anionic adducts for the production of negative ion electrospray spectra from N-linked carbohydrates, J. Am. Soc. Mass Spectrom. 16 (2005) 622–630.
[35] D.J. Harvey, Fragmentation of negative ions from carbohydrates. Part 2: fragmentation of high-mannose N-linked glycans, J. Am. Soc. Mass Spectrom. 16 (2005) 631–646.
[36] D.J. Harvey, Fragmentation of negative ions from carbohydrates. Part 3: fragmentation of hybrid and complex N-linked glycans, J. Am. Soc. Mass Spectrom. 16 (2005) 647–659.
[37] R. Čmelík, M. Štikarovská, J. Chmelík, Different behavior of dextrans in positive-ion and negative-ion mass spectrometry, J. Mass Spectrom. 39 (2004) 1467–1473.
[38] R. Čmelík, J. Chmelík, Structural analysis and differentiation of reducing and nonreducing neutral model starch oligosaccharides by negative-ion electrospray ionization ion-trap mass spectrometry, Int. J. Mass Spectrom. 291 (2010) 33–40.
[39] S.S. Choi, J.C. Kim, Influence of alkali metal cation type on ionization characteristics of carbohydrates in ESI-MS, Bull. Korean Chem. Soc. 30 (2009) 1996–2000.
[40] S.S. Choi, H.M. Lee, Analysis of mixture of maltooligoses using MALDI-TOFMS: influence of cationizing agent types, Bull. Korean Chem. Soc. 30 (2009) 2806–2808.
[41] D.J. Harvey, K. Baruah, C.N. Scanlan, Application of negative ion MS/MS to the identification of *N*-glycans released from carcinoembryonic antigen cell adhesion molecule 1 (CEACAM1), J. Mass Spectrom. 44 (2009) 50–60.
[42] G. Ritchie, D.J. Harvey, U. Stroeher, F. Feldmann, H. Feldmann, V. Wahl-Jensen, L. Royle, R.A. Dwek, P.M. Rudd, Identification of *N*-glycans from Ebola virus glycoproteins by matrix-assisted laser desorption/ionisation time-of-flight and negative ion electrospray tandem mass spectrometry, Rapid Commun. Mass Spectrom. 24 (2010) 571–585.
[43] G. Ritchie, D.J. Harvey, F. Feldmann, U. Stroeher, H. Feldmann, L. Royle, R.A. Dwek, P.M. Rudd, Identification of *N*-linked carbohydrates from severe acute respiratory syndrome (SARS) spike glycoprotein, Virology 399 (2010) 257–269.
[44] K.E. Andersen, C. Bjergegaard, P. Moller, J.C. Sorensen, H. Sorensen, Compositional variations for alpha-galactosides in different species of Leguminosae, Brassicaceae, and barley: a chemotaxonomic study based on chemometrics and high-performance capillary electrophoresis, J. Agric. Food Chem. 53 (2005) 5809–5817.
[45] L. Haska, M. Nyman, R. Andersson, Distribution and characterisation of fructan in wheat milling fractions, J. Cereal Sci. 48 (2008) 768–774.

[46] E. Vinogradov, K. Bock, Structural determination of some new oligosaccharides and analysis of the branching pattern of isomaltooligosaccharides from beer, Carbohydr. Res. 309 (1998) 57–64.
[47] C. Bruggink, M. Wuhrer, C.A.M. Koeleman, V. Barreto, Y. Liu, C. Pohl, A. Ingendoh, C.H. Hokke, A.M. Deelder, Oligosaccharide analysis by capillary-scale high-pH anion-exchange chromatography with on-line ion-trap mass spectrometry, J. Chromatogr. B. 829 (2005) 136–143.
[48] T.L. Constantopoulos, G.S. Jackson, C.G. Enke, Effects of salt concentration on analyte response using electrospray ionization mass spectrometry, J. Am. Soc. Mass Spectrom. 10 (1999) 625–634.
[49] P. Lehtonen, R. Hurme, Liquid-chromatographic determination of sugars in beer by evaporative light-scattering detection, J. Inst. Brew. 100 (1994) 343–346.